



# The interrelationship between LST, NDVI, NDBI, and land cover change in a section of Lagos metropolis, Nigeria

Alfred S. Alademomi<sup>1,2,3</sup> · Chukwuma J. Okolie<sup>1,2,3</sup> · Olagoke E. Daramola<sup>1,2</sup> · Samuel A. Akinnusi<sup>1,2</sup> · Elias Adediran<sup>1,2</sup> · Hamed O. Olanrewaju<sup>1,2</sup> · Abiodun O. Alabi<sup>1,2</sup> · Tosin J. Salami<sup>1,2</sup> · Joseph Odumosu<sup>2,4</sup>

Received: 26 November 2021 / Accepted: 22 March 2022 / Published online: 6 April 2022

© The Author(s), under exclusive licence to Società Italiana di Fotogrammetria e Topografia (SIFET) 2022, corrected publication 2022

## Abstract

In recent times, there has been renewed interest in understanding the dynamics of land cover change and its relationship with several environmental parameters. This study assesses the interrelationship between land surface temperature (LST), normalized difference vegetation index (NDVI), normalized difference built-up index (NDBI), and land cover change in Amuwo-Odofin Local Government Area of Lagos State, Nigeria. Multi-temporal and multi-spectral Landsat imageries for years 2002, 2013, 2016, and 2019 served as the primary dataset. Using the parallelepiped classifier, the imageries were classified into five land cover classes — mixed vegetation, bare land, built-up area, water body, and wetland. The spectral indices (NDVI and NDBI) were computed and the LST was determined using a single-channel algorithm. Land cover transition matrices were calculated to examine the proportion of land cover change between classes, including the unchanged areas. Pearson's correlation analysis enabled an analysis of the interdependence or interrelationship in the distribution of the parameters. From 2002 to 2019, the highest land cover transitions recorded were bare land to built-up area (12.64 km<sup>2</sup>), mixed vegetation to built-up area (21.55 km<sup>2</sup>), wetland to mixed vegetation (8.87 km<sup>2</sup>), and mixed vegetation to bare land (8.46 km<sup>2</sup>). There was a negative correlation between LST and NDVI, and between NDVI and NDBI. The distribution of the LST, NDVI, and NDBI varied correspondingly in accordance with land cover changes. The increase in built-up area could be the major driver of the observed changes in LST, NDBI, and NDVI, with an observed relationship that NDBI and LST values increase with increase in built-up areas.

**Keywords** Land cover · Land cover transition matrix · Land surface temperature · Normalized difference vegetation index · Normalized difference built-up index

## Introduction

In recent times, there has been renewed interest in understanding the dynamics of land cover change and its relationship with several environmental parameters. Some of

these key environmental parameters that have received the attention of researchers include the land surface temperature (LST), normalized difference vegetation index (NDVI), and normalized difference built-up index (NDBI) (Grigoraş and Urişescu 2019; Jaber 2019; Guha et al. 2020). These three parameters (LST, NDVI, and NDBI) are integral in the study and monitoring of land cover change (e.g., Zha et al. 2003; Deng et al. 2018; Alademomi et al. 2020). However, very few studies have investigated the link between LST, NDVI, NDBI, and land cover, and more studies are required to explore their interrelationship. Environmental parameters of relevance to human population and sustainability within an environment are mainly climatic factors which are easily influenced by land cover practices and the same holds for the reverse (Guha et al. 2018; Malik et al. 2019).

According to the United Nations Population Fund (UNFPA 2020), the planet is witnessing the biggest urban

✉ Abiodun O. Alabi  
aoalabi@unilag.edu.ng

<sup>1</sup> Department of Surveying and Geoinformatics, Faculty of Engineering, University of Lagos, Lagos, Nigeria

<sup>2</sup> Geospatial and Environmental Research Group, University of Lagos, Lagos, Nigeria

<sup>3</sup> Centre for Multidisciplinary Research and Innovation (CEMRI), Abuja, Nigeria

<sup>4</sup> Department of Surveying and Geoinformatics, School of Environmental Technology, Federal University of Technology, Minna, Niger State, Nigeria

growth wave in history. More than half of the world's population now live in cities and towns, and this figure will rise to about 5 billion by 2030 (UNFPA 2020). As a result, this urbanization growth has emerged as a primary driving force of demographic, social, economic, and environmental changes (Choudhury et al. 2019). For example, there has been an increase in the rate of conversion of non-built-up area to impervious land and as well as changing scenario of general landscape due to population explosion and increase in the demand for urban expansion worldwide (Das et al. 2020). Due to urban growth, rapid change of land use/land cover (LULC) profoundly affects biodiversity and ecosystem function, as well as local and regional climate (Choudhury et al. 2019). Because of the fast alterations, the changes in land use will affect the degree of solar radiation absorption, surface temperature, evaporation rate, heat soil transfer, heat storage, and wind turbulence (Hua and Ping 2018).

Land Surface Temperature (LST) refers to the solar radiation-derived radiative skin temperature of the land (Jaber 2019). It is a measure of how hot the earth's surface would feel to touch at specific spots which usually vary with land cover/land use type. According to Obiefuna et al. (2018), LST is one of the key environmental parameters that is affected by changes in land cover. For many fields, measuring LST is significant, including climate variability and change, urban heat island impact, land/atmosphere feedback, fire monitoring, mapping and detection of land cover and change, geological studies, crop management, and water management (Jaber 2019). LST can provide information on the physical characteristics of the soil surface and climatic conditions, as well as changes in land use and human activities that affect the climate (Fathizad et al. 2017). Land use purposes such as buildings, roads, and industries are known to be the impervious surface that, on the one hand, can absorb shortwave incoming solar radiation but, on the other hand, contribute to a decrease in outgoing longwave terrestrial emissions which in turn have direct impact on the LST (Das et al. 2020). The information of LST is crucial to the understanding of different environmental complexities. However, due to the surface heterogeneity induced by the numerous land cover and mixed uses, LST estimation is complicated. This is because the emissivity of land surfaces is highly variable and can differ over short distances (Akinbobola 2019; Akinyemi et al. 2019). Various forms of land cover affect the nature and distribution of the LST, and because of this, Guha et al. (2020) inferred from their study that seasonal fluctuations in LST are primarily dependent on elements of vegetation and temperature. Although it is known that vegetation cover reduces LST, yet vegetation types can vary in their ability to reduce the temperature of the surface. In addition to

evapotranspiration, trees minimize surface and air temperature by shading (Alexander 2020).

A spectral index for detecting long-term differences in vegetation coverage and its status is the Normalized Difference Vegetation Index (NDVI) (Fathizad et al. 2017). With values ranging from  $-1$  to  $+1$ , NDVI shows the condition and abundance of the green vegetation cover and biomass. The higher the values and closer to 1, the denser and healthier the vegetation on the ground and the non-vegetated surfaces are shown by zero or negative values (Jaber 2019). NDVI is used to quantify vegetation greenness and is useful in understanding vegetation density and assessing changes in plant health. The NDVI is one of the most widely used indices for regional and global monitoring of vegetation dynamics. This index essentially reflects greenness, where negative values are derived primarily from clouds, water, and snow, and values close to zero are formed primarily from bare soil and rocks. The NDVI functions with very small values (0.1 or less) corresponding to empty areas of rock, sand, or snow. Shrubs and meadows are characterized by moderate values (from 0.2 to 0.3), while high values (from 0.6 to 0.8) reflect temperate and tropical forests. This scale is successfully used for crop monitoring to show farmers which parts of their fields at any given moment have dense, moderate, or sparse vegetation. Studies have shown that there is a logical relationship between NDVI and LST (Fathizad et al. 2017; Marzban et al. 2018; Jaber 2019; Guha et al. 2020; Alademomi et al. 2020).

Another interesting spectral index is the Normalized Difference Built-up Index (NDBI), which gives information on extent of urbanization in a region as well as the land cover change. This parameter has been found to exhibit good correlation with LST (Choudhury et al. 2019; Das et al. 2020; Guha et al. 2020). NDBI values range from  $-1$  to  $+1$  with higher values indicating presence of more impervious surface and vice versa. On a local scale, the expansion of built-up/impervious areas alters the physical and geometrical characteristics of a land surface compared to natural land cover, resulting in surface energy alteration and radiation budgets (Choudhury et al. 2019). The presence of impervious surfaces such as buildings, roads, and industrial farms increases shortwave radiation absorption and reduces energy loss due to longwave radiation emission (Choudhury et al. 2019; Das et al. 2020). Consequently, these impervious surfaces will have higher LST compared to the surrounding environment. NDBI like other spectral indices which quantitatively represent LULC type have been used widely in LST-LULC studies; however, the seasonal variability of the correlation between LST and NDBI is still an area of concern. NDBI plays an important role in urban areas where most of the human population are concentrated (Guha et al. 2018).

Researchers have adopted different approaches to examine the relationship between LST, land cover, and NDVI. Guha et al. (2020) estimated the LST of Raipur City in India and the relationship with NDVI, normalized difference water index (NDWI), NDBI, and normalized multi-band drought index using four multi-date Landsat 8 images acquired at different seasons. Their work showed a weak correlation between LST and the spectral indices in the winter and pre-monsoon images while the strongest correlation was in monsoon and post-monsoon images. Fathizad et al. (2017) investigated the spatiotemporal variability of LST in the desert region of Dasht-e-Abbas, Ilam, Iran, using Landsat images. Their findings indicated a rise in LST in areas where improvements in deforestation, land use, and land cover had taken place. Alexander (2020) combined NDVI estimated from Landsat 8 thermal band with different land cover types derived from airborne Light detection and ranging (LiDAR) data to understand LST in Aarhus city, Denmark. Their results showed that tree cover and building cover contribute more to the variation of LST compared to the surrounding vegetation cover in the study area. In Grigoraş and Urişescu (2019), NDVI was used to model the relationship between land cover and LST to understand their impact on surface urban heat island in the summer season between 1984 and 2016. Over the period of the study, their results showed evidence of increased urbanization and its contribution to the urban heat island (UHI) in the region. Jaber (2019) used the MODIS (Moderate Resolution Imaging Spectrometer) dataset to analyze the effect of land cover on the relationship between daytime and nighttime LST. The findings showed that land cover accounted for a fair amount of NDVI variability, but a small amount of LST daytime and nighttime variability. Nse et al. (2020) evaluated the relationship between LST, land cover, and NDVI from Landsat images using the contribution index (CI) and Pearson's correlation analysis. The study discovered that the highest contribution to LST was the built-up area. In another study, Babalola and Akinsanola (2016) assessed the spatial distribution of land cover and LST changes in Lagos metropolis, Nigeria. UHI in the region has been greatly influenced by the increase in urbanization activities and the reduction in natural vegetation as reported in their study. The influence of land cover changes on LST in the rapidly urbanizing metropolis of Lagos was investigated by Obiefuna et al. (2018) between 1984 and 2015 using multi-temporal Landsat imagery. Their findings showed that the rapid urbanization in the metropolis of Lagos altered the thermal surface environment as shown by increased LST. Using Landsat-derived data on land cover, LST, and vegetation indices, Alademomi et al. (2020) estimated the magnitude of environmental changes in the Lagos Lagoon environment. Their analysis showed an increase in LST, with the built-up areas having the highest contribution while

wetlands and other vegetated areas had the least impact on LST variability.

Siqi and Yuhong (2020) analyzed the patterns of LST and land cover in Hong Kong and their seasonal variability using NDVI, NDBI, NDBal, and NDWI. The results indicated that LST is significantly affected by land cover types with good positive correlation between LST, NDBI, and NDBal and negative correlation between LST, NDVI, and NDWI. It was also reported that the magnitudes of the influences of indices vary with the season. The correlation coefficients of above-mentioned relationships were more significant in summer season (May, August, September). More so, Choudhury et al. (2019), examined the influence of land use/land cover (LULC) on land surface temperature using spectral indices including NDVI, NDBI, and NDWI in Asansol-Durgapur Development Region, India. It was observed that impervious surfaces largely contributed to the LST compared to other land cover types and that the rate of change of LST in winter was lower compared to what was observed in summer. On the contrary, Das et al. (2020) showed that the LST changed drastically over a 23-year study period in Asansol subdivision, India, but the rate of change was higher in winter season than summer season. Generally, there was negative correlation between LST and NDVI and NDWI while a positive good correlation was recorded between LST and NDBI (Choudhury et al. 2019; Das et al. 2020). In the overview, research has shown that LST is increasing generally in various communities of the world due to the increase in human population and human activities.

This study is focused on the assessment of the inter-relationship between LST, NDVI, NDBI, and land cover change using multi-spectral Landsat imageries for 2002, 2013, 2016, and 2019. The objectives are as follows: (i) supervised image classification of the Landsat image-ries; (ii) accuracy assessment of the image classifica-tion; (iii) calculation of the spectral indices: NDVI and NDBI; (iv) determination of the LST using the Landsat thermal bands and a single-channel algorithm; and (v) assessment of the correlation between LST, NDVI, and NDBI, and the relationship with land cover changes. The findings of this study contribute to the body of knowl-edge on land cover change dynamics, and global and environmental change.

## Materials and methods

### Study area

The study area is Amuwo Odofin (shown in Fig. 1), one of the Local Government Areas (LGAs) in Lagos State,

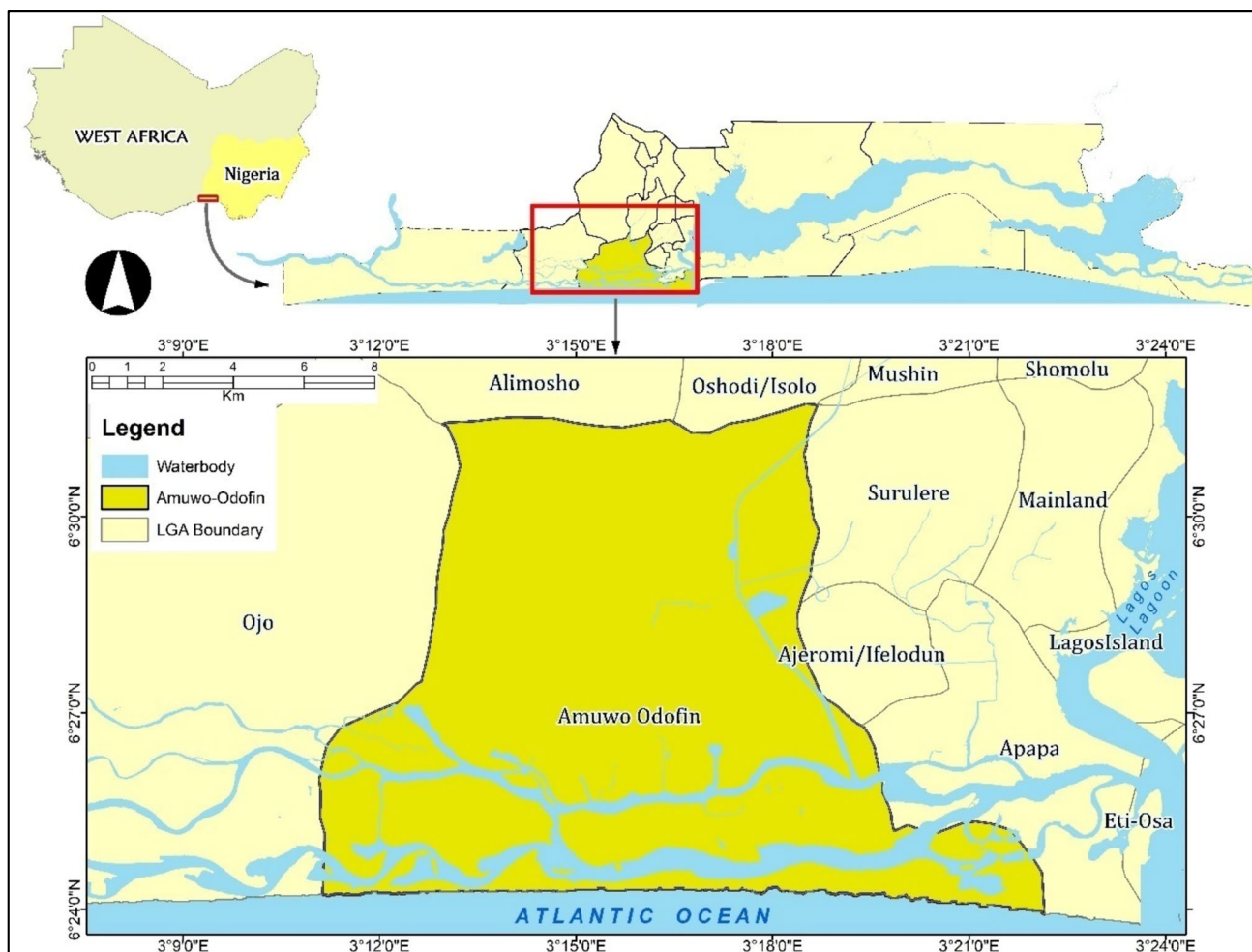


**Fig. 1** Map showing the location of Amuwo Odofin LGA

Nigeria. It covers an area of about 173 km<sup>2</sup> and is located within the metropolitan area of Lagos. According to the 2006 Nigerian population census, Amuwo Odofin LGA has a population of over 524,971 and this figure was expected to rise to 766,111 in 2018 and over a million in 2021 (Lagos Bureau of Statistics 2019). The LGA shares borders with Ajeromi-Ifelodun, Surulere and Apapa LGAs to the east, Ojo LGA to the west, the Atlantic Ocean to the south, and Alimosho and Oshodi/Isolo LGAs to the north. Two air masses influence the climate of the area: the tropical maritime and tropical continental air masses. The former is wet and originates from the Atlantic Ocean, while the latter originates from the Sahara Desert and is warm, dry, and dusty. The two main seasons recognized in the region are as follows: the dry season (between November and March) and the rainy season (between April and October), with a brief break in the middle of August. Amuwo Odofin is divided into two distinct geographical spheres of riverine areas and upland. The area is richly blessed with mangroves and varieties of coastal wetlands.

### Landsat imagery

The Landsat program is a series of Earth-observing satellite missions jointly managed by the National Aeronautics and Space Administration (NASA) and the United States Geological Survey (USGS) to provide a global and continuous remote sensing of the earth's resources. Since 1972, Landsat satellites have collected information about Earth from space. The products of this program are freely accessible and of immense value to many potential users. The Earth observing instrument on Landsat 7, the Enhanced Thematic Mapper Plus (ETM+), is an improvement over the capabilities of the highly successful Thematic Mapper instruments on Landsat 4 and 5. The Landsat 8 satellite payload consists of two science instruments — the Operational Land Imager (OLI) and the Thermal InfraRed Sensor (TIRS). These two sensors provide seasonal coverage of the global landmass at a spatial resolution of 30 m (visible, near infrared and shortwave infrared); 100 m (thermal); and 15 m (panchromatic). The Landsat data for



**Table 1** Characteristics of the Landsat imageries used for the study

Dataset	Path/row	Date of acquisition (DD-MM-YYYY)	Time (GMT)
Landsat 7 ETM+	191/55	28-12-2002	9:51:41
Landsat 8 OLI		18-12-2013	10:04:25
		26-12-2016	10:03:10
		01-01-2019	10:02:48

this study covered the dry season period in Lagos State and were downloaded from USGS Earth Explorer (<https://earthexplorer.usgs.gov/>). Landsat Level 2 products were ordered and downloaded from the USGS Earth Resources Observation and Science (EROS) Centre Earth Science Processing Architecture on-demand interface. Table 1 shows the characteristics of the Landsat imageries used.

**Image pre-processing and enhancement**

The Landsat imageries were combined into false color composites within the ENVI 5.2 software environment using the

following band combinations: 5–4–3 for Landsat 8 OLI and 4–3–2 for Landsat 7 ETM+. Thereafter, the Gram-Schmidt spectral sharpening algorithm was used to pansharpener the image composite using the panchromatic band. This improved spatial resolution from 30 to 15 m thereby enhancing interpretation. The Gram-Schmidt method gives accurate results and is recommended for most applications (L3Harris Geospatial 2020).

**Land cover, NDVI, NDBI, and LST**

Using the parallelepiped supervised classification algorithm, the Landsat imageries were classified into 5 information classes — mixed vegetation, bare land, built-up area, water body, and wetland. The theoretical background of parallelepiped classification is already well explained in the extant literature (e.g., Obiefuna et al. 2021). After classification, the features were converted to ESRI shapefile format for further editing. Land cover transition matrices were calculated to examine the proportion of land cover change between classes, including the unchanged areas. This was done with the Intersect tool in Arc Toolbox. The intersect table was

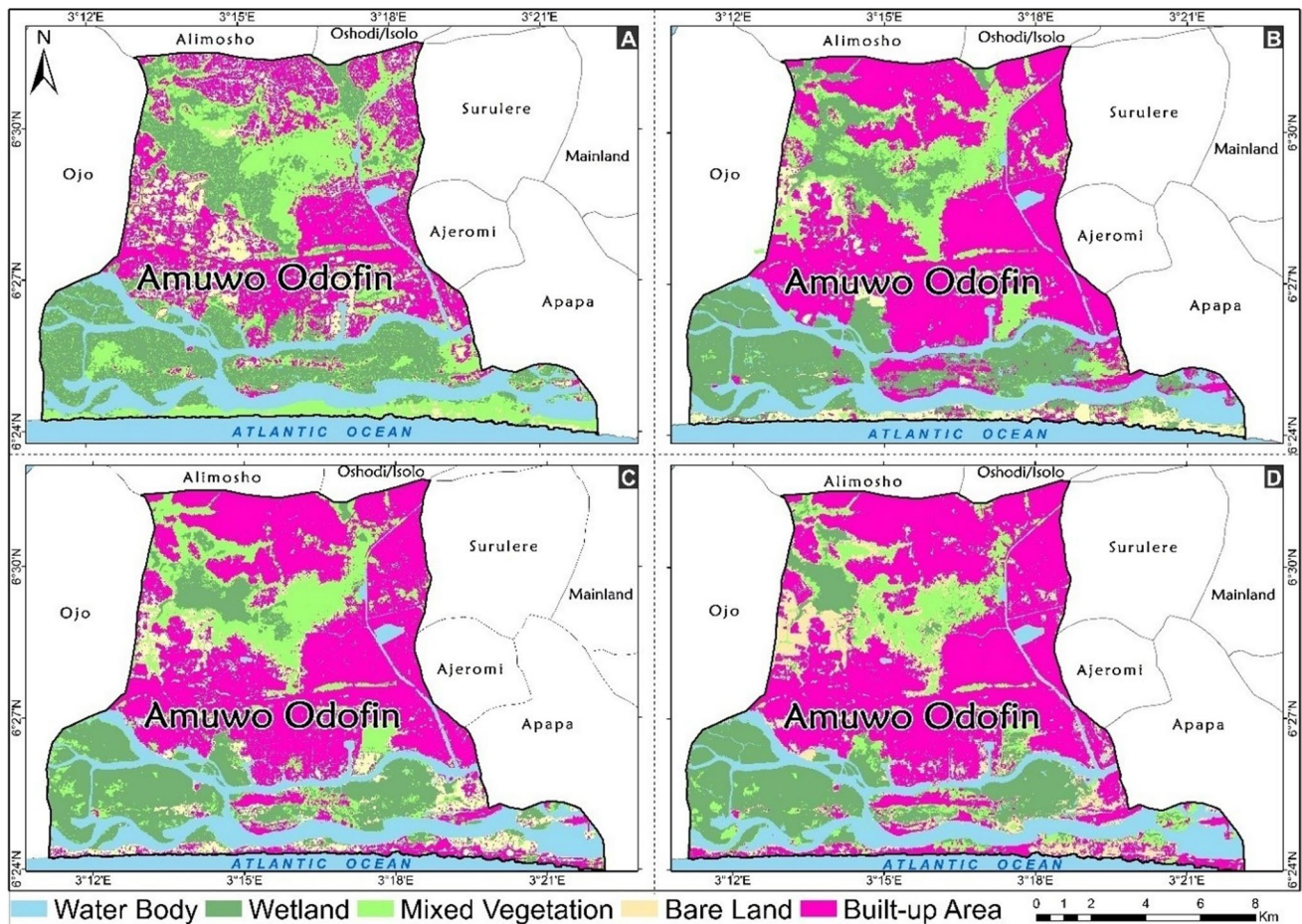


**Fig. 2** Maps showing distribution of land cover. **a** 2002, **b** 2013, **c** 2016, and **d** 2019

**Table 2** Coverage area of land cover classes in Amuwo Odofin LGA, 2002–2019

Land cover	Area, 2002		Area, 2013		Area, 2016		Area, 2019	
	km <sup>2</sup>	%	km <sup>2</sup>	%	km <sup>2</sup>	%	km <sup>2</sup>	%
Bare land	15.12	8.73	11.26	6.5	16.02	9.25	20	11.55
Built-up area	46.78	27	74.34	42.92	76.0	43.87	81.09	46.81
Mixed vegetation	44.93	25.94	23.74	13.71	25.7	14.84	18.88	10.9
Water body	23.82	13.75	22.84	13.18	23.02	13.29	22.73	13.12
Wetland	42.58	24.58	41.04	23.69	32.48	18.75	30.53	17.63
Total	173.23	100	173.22	100	173.22	100	173.23	100

transferred to Microsoft Excel where it was analyzed using pivot tables.

The NDVI is computed as the difference between the near-infrared (NIR) and red (RED) spectral reflectance bands divided by their sum. The NDBI is calculated as a ratio between the shortwave infrared (SWIR) and near infrared (NIR) values in traditional fashion.

$$\text{NDVI} = \frac{\text{NIR} - \text{RED}}{\text{NIR} + \text{RED}} \quad (1)$$

$$\text{NDBI} = \frac{\text{SWIR} - \text{NIR}}{\text{SWIR} + \text{NIR}} \quad (2)$$

where,

Red = Band 4 (Landsat 8 OLI) or Band 3 (Landsat 7 ETM+).

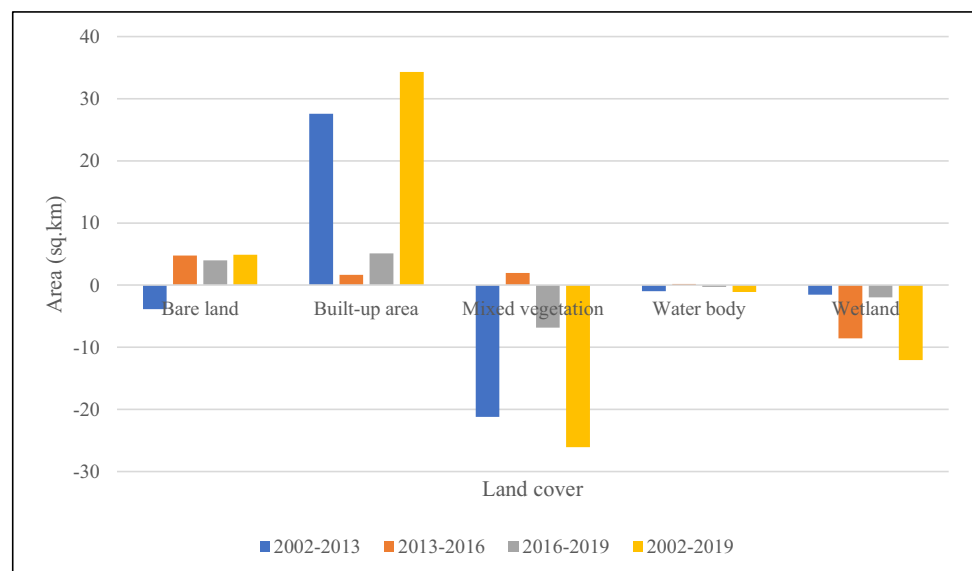
NIR = Band 5 (Landsat 8 OLI) or Band 4 (Landsat 7 ETM+).

SWIR = Band 6 (Landsat 8 OLI) or Band 5 (Landsat 7 ETM+).

The LST was computed using the single-channel algorithm (see Oguz 2013; Ferrelli et al. 2015; Alademomi et al. 2020; Obiefuna et al. 2018, 2021). Landsat 7 ETM+ Band 6\_1 and Landsat 8 TIRS Band 10 were used for the retrieval. This basically involves the following steps: (i) conversion of digital number to spectral radiance (USGS 2015; Zareie et al. 2016), (ii) conversion of spectral radiance to top-of-atmosphere brightness temperature (Schott and Volchok 1985; Wukelic et al. 1989; Qin et al. 2001; Zareie et al. 2016), and (iii) conversion of brightness temperature to LST (Weng et al. 2004; Cummings 2007; Zareie et al. 2016).

### Quantitative analysis

The minimum level of interpretation accuracy in the classification of land cover classes from remotely sensed data should be at least 85% (Anderson 1971; Alademomi et al. 2020). An accuracy assessment was done by comparing the interpreted features on imagery and their corresponding classification outputs. The kappa coefficient and overall accuracy were calculated. The classified data was converted

**Fig. 3** Areal changes in land cover

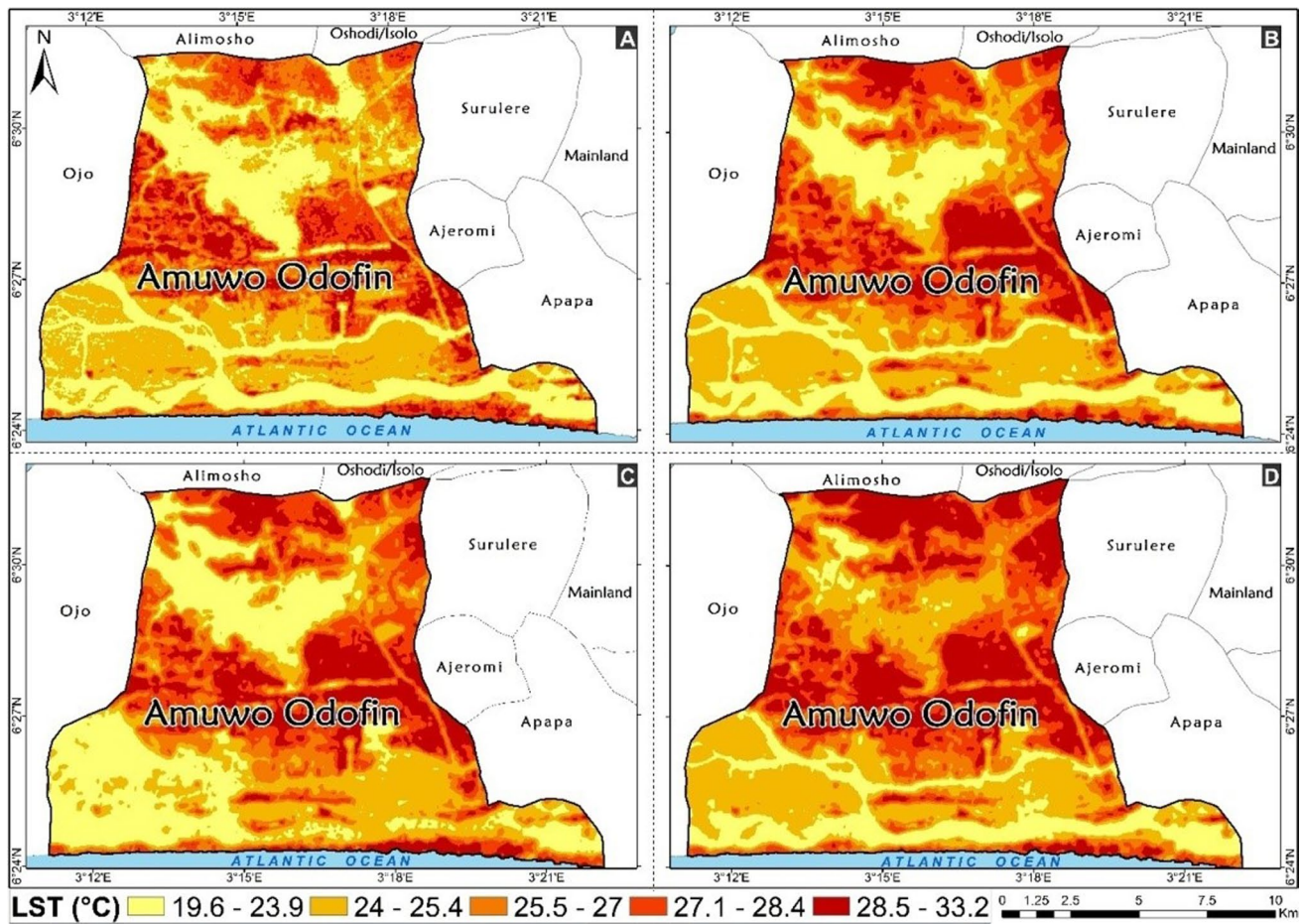


Fig. 4 Maps showing distribution of LST. a 2002, b 2013, c 2016, and d 2019

Table 3 Accuracy assessment results

Year	Overall accuracy (%)	Kappa coefficient
2002	82.14	0.7727
2013	87.89	0.8443
2016	95.56	0.9440
2019	93.16	0.9143

from polygon to raster format using the polygon to raster tool in ArcGIS. Afterwards, 200 random points were created using the ArcGIS Fishnet tool and spread across the Landsat imageries covering the different classes. The attribute table of these points were populated with class codes corresponding to the different land cover classes which they coincided with. The kappa coefficient and overall accuracy of classification were then calculated with the following formulae (Das and Angadi 2020):

Table 4 Transition matrix of land cover change (in km<sup>2</sup>) from 2002 to 2013

Land cover class		2013					Total
		Bare land	Built-up area	Mixed vegetation	Waterbody	Wetland	
2002	Bare land	2.50	11.89	0.62	0.00	0.11	15.12
	Built-up area	1.97	41.29	2.91	0.05	0.55	46.78
	Mixed vegetation	5.79	15.67	12.93	0.60	9.94	44.93
	Water body	0.28	1.30	0.39	20.83	1.01	23.82
	Wetland	0.72	4.19	6.83	1.36	29.47	42.56
Total		11.26	74.34	23.69	22.84	41.08	173.21



**Table 5** Transition matrix of land cover change (in km<sup>2</sup>) from 2013 to 2016

Land cover class		2016					Total
		Bare land	Built-up area	Mixed vegetation	Waterbody	Wetland	
2013	Bare land	3.52	6.12	1.23	0.19	0.21	11.26
	Built-up area	4.55	66.07	1.78	1.32	0.61	74.34
	Mixed vegetation	4.38	3.13	13.47	0.22	2.48	23.69
	Waterbody	0.34	0.12	0.41	20.97	1.00	22.84
	Wetland	3.23	0.52	8.81	0.34	28.17	41.08
	Total	16.02	75.97	25.70	23.04	32.48	173.21

**Table 6** Transition matrix of land cover change (in km<sup>2</sup>) from 2016 to 2019

Land cover class		2019					Total
		Bare land	Built-up area	Mixed vegetation	Waterbody	Wetland	
2016	Bare land	6.46	6.03	1.97	0.34	1.24	16.02
	Built-up area	4.74	70.64	0.46	0.12	0.01	75.97
	Mixed vegetation	6.35	3.66	11.11	0.24	4.33	25.70
	Water body	0.73	0.22	0.40	21.47	0.21	23.04
	Wetland	1.73	0.52	4.93	0.56	24.74	32.48
	Total	20.00	81.07	18.88	22.73	30.53	173.21

**Table 7** Transition matrix of land cover change (in km<sup>2</sup>) from 2002 to 2019

Land cover class		2019					Total
		Bare land	Built-up area	Mixed vegetation	Waterbody	Wetland	
2002	Bare land	2.31	12.64	0.14	0.01	0.02	15.12
	Built-up area	3.94	41.76	0.63	0.11	0.33	46.78
	Mixed vegetation	8.46	21.55	8.81	0.67	5.43	44.93
	Water body	0.78	0.43	0.56	20.96	1.09	23.82
	Wetland	4.52	4.69	8.72	0.97	23.67	42.56
	Total	20.00	81.07	18.88	22.73	30.53	173.21

$$k = \frac{N \sum_{i=1}^r X_{ii} - \sum_{i=1}^r (X_{i+} * X_{+i})}{N^2 - \sum_{i=1}^r (X_{i+} * X_{+i})} \tag{3}$$

Where:

*r* = number of rows and columns in error matrix

*N* = total number of observation (pixels)

*X<sub>ii</sub>* = observation in row *i* and column *i*

*X<sub>i+</sub>* = marginal total of row *i*

*X<sub>+i</sub>* = marginal total of column *i*

*k* = Kappa coefficient

$$\text{Overall accuracy} = \frac{\text{Total number of correct samples}}{\text{Total number of samples}} \times 100 \tag{4}$$

Descriptive statistics and correlation analysis were performed in Microsoft Excel to understand the relationship between the LST, NDVI, NDBI, and land cover. The Pearson’s correlation analysis enabled an analysis of the interdependence or interrelationship in the distribution of the

parameters. The Pearson’s correlation coefficient is represented with the formula below (Nwilo et al. 2020):

$$r = \frac{\sum (x_i - \bar{x})(y_i - \bar{y})}{\sqrt{\sum (x_i - \bar{x})^2 \sum (y_i - \bar{y})^2}} \tag{5}$$

*x<sub>i</sub>* = values of the *x* – variable in the sample

$\bar{x}$  = mean of the values of the *x* – variables

*y<sub>i</sub>* = values of the *y* – variable in the sample

$\bar{y}$  = mean of the values of the *y* – variables

*r* = correlation coefficient

## Results and analysis

### Analysis of land cover change

Figure 2 shows the land cover maps while Table 2 presents the coverage area of land cover classes in Amuwo Odofin



LGA between 2002 and 2019. There was a very large increase in the extent of built-up area between 2002 and 2019. Between 2002 and 2013, the built-up areas increased at a rate of 2.5 km<sup>2</sup>/year from 46.78 km<sup>2</sup> to 74.34 km<sup>2</sup>. Between 2013 and 2016, the built-up areas increased at the rate of 0.5 km<sup>2</sup>/year, and by 1.7 km<sup>2</sup>/year between 2016 and 2019. This resulted in an expansion of built-up areas from 74.34 km<sup>2</sup> in 2013 to 81.09 km<sup>2</sup> in 2019. Bare lands declined from 15.12 km<sup>2</sup> to 11.26 km<sup>2</sup> between 2002 and 2013. However, between 2013 and 2019, it increased at the rate of 1.4 km<sup>2</sup>/year; from 11.26 km<sup>2</sup> in 2013 to 16.02 km<sup>2</sup> in 2016 and to 20 km<sup>2</sup> in 2019. A possible reason for the increase in bare land could be due to several sand filling and land reclamation projects that were embarked upon by the Lagos State Government during this period. Also, there were several cases of buildings that were demolished for encroaching into the right-of-way of the expanded Mile 2 — Badagry expressway. There are several open fields at road junctions, transportation parks, and within residential areas (see Plate 1). Between 2002 and 2013, the wetlands decreased at the rate of 0.14 km<sup>2</sup>/year from 42.58 km<sup>2</sup> to 41.04 km<sup>2</sup>.

Subsequently, the coverage reduced at a rate of 2.8 km<sup>2</sup>/year to 32.48 km<sup>2</sup> in 2016, and further declined at the rate of 0.65 km<sup>2</sup>/year to 30.53 km<sup>2</sup> in 2019. Similarly, there was an overall decrease in the vegetation cover between 2002 and 2019. At a rate of 2 km<sup>2</sup>/year, the vegetation cover declined from 44.93 km<sup>2</sup> in 2002 to 23.74 km<sup>2</sup> in 2013. It subsequently increased between 2013 and 2016 from 23.74 km<sup>2</sup> to 25.7 km<sup>2</sup> but reduced to 18.88 km<sup>2</sup> in 2019. Between 2002 and 2019, the vegetation reduced from 44.93 km<sup>2</sup> to 18.88 km<sup>2</sup>. The coverage of water body decreased from 23.82 km<sup>2</sup> to 22.84 km<sup>2</sup> between 2002 and 2013. It increased slightly by 0.18 km<sup>2</sup> between 2013 and 2016 and further decreased by 0.29 km<sup>2</sup> between 2016 and 2019.

Figure 3 shows areal changes in land cover. Between 2002 and 2019, there was a net increase of 4.88 km<sup>2</sup> in bare lands and 34.31 km<sup>2</sup> in built-up areas, and a net decrease of 26.05 km<sup>2</sup> in mixed vegetation, 1.09 km<sup>2</sup> in water bodies, and 12.05 km<sup>2</sup> in wetlands.

The results of the land cover classification were validated through accuracy assessment analysis as shown in Table 3. The overall accuracy was lowest in 2002 and highest in

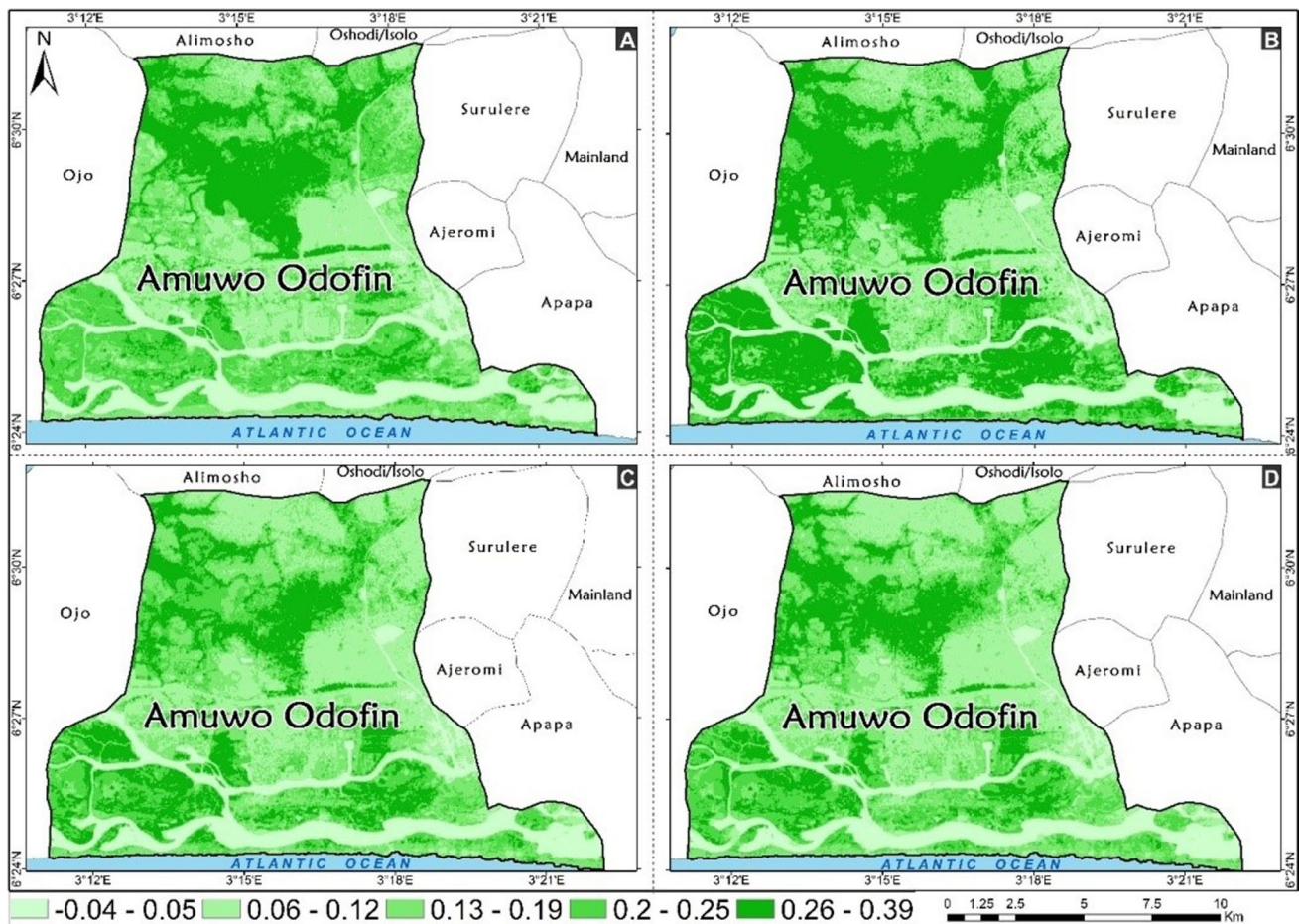


Fig. 5 Maps showing distribution of NDVI. a 2002, b 2013, c 2016, and d 2019

2016. The improvements in Landsat 8 OLI image over Landsat 7 ETM+ image could be the reason for the higher accuracies observed for 2013, 2016, and 2019.

### Transition matrix of land cover change

The transition matrix displays the number of different forms of land cover that have either remained unchanged or changed over the study periods. Tables 4, 5, 6, and 7 present the land cover transition matrices between the periods 2002–2013, 2013–2016, 2016–2019, and 2002–2019, respectively. The highest transition between 2002 and 2013 occurred with the built-up area which gained a combined sum of 27.56 km<sup>2</sup> from mixed vegetation (15.67 km<sup>2</sup>) and bare land (11.89 km<sup>2</sup>). Within the same period, about 10 km<sup>2</sup> of mixed vegetation was converted to wetland; 5.79 km<sup>2</sup> of mixed vegetation and 1.97 km<sup>2</sup> of built-up area were converted to bare land. Also, 2.91 km<sup>2</sup> of built-up area and 6.83 km<sup>2</sup> of wetland were converted to mixed vegetation. Water body scarcely changed within the period as 1.30 km<sup>2</sup> and 1.01 km<sup>2</sup> were converted to built-up area and wetland,

respectively. For the periods of 2013–2016 and 2016–2019 (Tables 5 and 6), there were several low transitions. Between 2013 and 2016, 8.81 km<sup>2</sup> of wetland changed to mixed vegetation, 6.12 km<sup>2</sup> of bare land changed to built-up area, 4.55 km<sup>2</sup> of built-up area changed to bare land, and 4.38 km<sup>2</sup> of mixed vegetation was converted to bare land.

Between 2016 and 2019, the significant transitions were bare land to built-up area (6.03 km<sup>2</sup>), mixed vegetation to bare land (6.35 km<sup>2</sup>), wetland to mixed vegetation (4.93 km<sup>2</sup>), built-up area to bare land (4.74 km<sup>2</sup>), and mixed vegetation to wetland (4.33 km<sup>2</sup>). From 2002 to 2019, the highest transitions recorded were bare land to built-up area (12.64 km<sup>2</sup>), mixed vegetation to built-up area (21.55 km<sup>2</sup>), wetland to mixed vegetation (8.72 km<sup>2</sup>), and mixed vegetation to bare land (8.46 km<sup>2</sup>). Other transitions in the period include wetland to bare land (4.52 km<sup>2</sup>), wetland to built-up area (4.69 km<sup>2</sup>), mixed vegetation to wetland (5.43 km<sup>2</sup>), built up area to bare land (3.94 km<sup>2</sup>), and water body to wetland (1.09 km<sup>2</sup>).

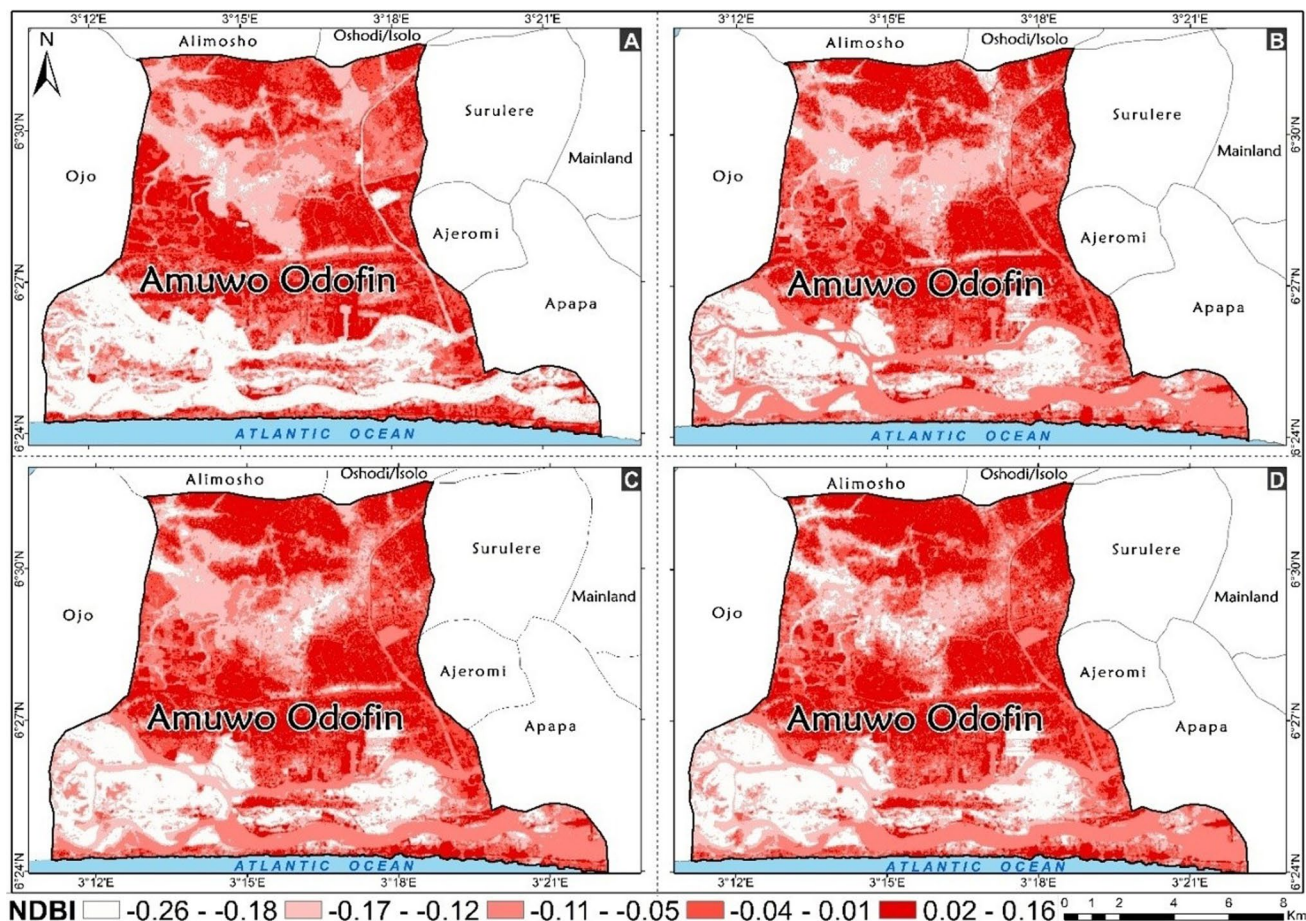


**Fig. 6** Maps showing distribution of NDBI. **a** 2002, **b** 2013, **c** 2016, and **d** 2019



**Plate 1** An open field adjacent to Alakija roundabout along Lagos-Badagry expressway in Amuwo-Odofin ( source: Field survey, 2021)



**Analysis of variation in LST, NDVI, and NDBI**

Figures 4, 5, and 6 show the distribution of LST, NDVI, and NDBI. The LST is observed to have increased in tandem with the expansion in built-up areas. This increase is most noticeable in the central and northern parts of the study area. Relatedly, the large expansion in built-up areas is associated with higher LST (Fig. 4), lower NDVI (Fig. 5), and higher NDBI (Fig. 6). The NDVI spatial distribution depicts an inverse pattern to LST and NDBI. The NDVI values are generally higher over mixed vegetation and wetland compared to other land cover types. The diminishing NDVI is partly attributable to the built-up area expansion which causes loss of vegetation and wetland cover. Table 8 presents the descriptive statistics of LST, NDVI, and NDBI for the Landsat 8-derived data (2013, 2016 and 2019) which were summarized from 2752 random points spread across the study area.

**Table 8** Descriptive statistics of NDVI, NDBI, and LST

Parameter	LST			NDVI			NDBI		
	2013	2016	2019	2013	2016	2019	2013	2016	2019
Mean	26.69	25.47	26.25	0.41	0.36	0.36	-0.14	-0.11	-0.10
Median	26.10	25.18	26.18	0.43	0.35	0.34	-0.16	-0.12	-0.10
Min	22.31	21.42	20.15	-0.12	-0.02	-0.03	-0.48	-0.44	-0.42
Max	33.05	31.24	32.06	0.80	0.67	0.73	0.20	0.20	0.19
Range	10.75	9.81	11.91	0.93	0.69	0.76	0.68	0.64	0.61

**Interrelationship between LST, NDVI, and NDBI**

Table 9 presents the coefficient of correlations between LST, NDVI, and NDBI for the Landsat-8 derived data (2013, 2016 and 2019). Generally, LST versus NDVI, and NDBI versus NDVI are negatively correlated. Conversely, there is a strong positive correlation between LST and NDBI with values ranging from 0.84–0.86 for all the years.

**Relationship between land cover, LST, NDVI, and NDBI**

Table 10 presents the descriptive statistics of LST, NDVI, and NDBI per land cover class for the Landsat 8-derived data (2013, 2016 and 2019). The highest mean LSTs are generally observed in built-up areas followed by bare land. The mean LST values for mixed vegetated and wetland areas are roughly in the same region with about 0.5 °C

**Table 9** Coefficient of correlation (r) between LST, NDVI, and NDBI

	LST 2013	LST 2016	LST 2019	NDVI 2013	NDVI 2016	NDVI 2019	NDBI 2013	NDBI 2016	NDBI 2019
<b>LST 2013</b>	1.00	0.95	0.93	-0.28	-0.38	-0.37	0.84	0.81	0.79
<b>LST 2016</b>	0.95	1.00	0.92	-0.42	-0.53	-0.51	0.86	0.87	0.84
<b>LST 2019</b>	0.93	0.92	1.00	-0.25	-0.38	-0.37	0.85	0.85	0.86
<b>NDVI 2013</b>	-0.28	-0.42	-0.25	1.00	0.95	0.92	-0.54	-0.52	-0.47
<b>NDVI 2016</b>	-0.38	-0.53	-0.38	0.95	1.00	0.96	-0.59	-0.63	-0.62
<b>NDVI 2019</b>	-0.37	-0.51	-0.37	0.92	0.96	1.00	1.00	0.94	-0.63
<b>NDBI 2013</b>	0.84	0.86	0.85	-0.54	-0.62	-0.59	1.00	0.94	0.92
<b>NDBI 2016</b>	0.81	0.87	0.85	-0.52	-0.67	-0.63	0.94	1.00	0.95
<b>NDBI 2019</b>	0.79	0.84	0.86	-0.47	-0.62	-0.63	0.92	0.95	1.00

difference in the mean LSTs. The mean NDVI is highest over wetland and mixed vegetation. This is indicative of the moderating effect of vegetation cover on LST. The mean NDBI values are mostly negative for almost all the land cover classes through the years the study covers. The highest is observed over bare land and built-up area while the lowest is recorded over wetland. Furthermore, it is observed in Table 9 that there exists a negative correlation between LST and NDVI in the years 2016 and 2019 with values of  $-0.53$  and  $-0.37$ , respectively. The positive relationship found between NDBI and LST suggests that built-up area is generating much surface temperature variations and perhaps one of the key contributors in urban heat island. This further indicates that the development of urban heat islands is detrimental to phonological process in the tropics (Kabano et al. 2021).

## Discussion

The observed increase in built-up area is in tandem with the findings of Obiefuna et al. (2018), Babalola and Akinsanola (2016), and Abiodun et al. (2005). All these studies examined the land cover changes in Lagos metropolis. Another reason for the rapid increase in the built-up area is the rate of population growth in the area. According to Yusuf et al. (2013), the population in Lagos grew from 9.3 million in 2006 to over 21 million in 2018. In Amuwo Odofin, the population was projected to be 697,000 in 2015 from 225,823 in 1991. Some densely populated areas of Amuwo Odofin include Alakija (Plate 2) and Festac Town (Plate 3). The decrease in bare lands between 2002 and 2013 agrees with the results of Abiodun et al. (2005) and Babalola and Akinsanola (2016). A possible explanation for this decrease is sand filling and conversion of vegetated area and wetland area into residential areas (Ajibola et al. 2012). The decline in wetlands is also corroborated by Obiefuna et al. (2013, 2013b, 2018) and Ajibola et al. (2012). Ajibola et al. (2012) posited that the loss of wetland in Lagos metropolis is as a result of human activities which include incessant sand filling and conversion of wetland environment to economic uses (through construction) and perennial flooding which is a common and regular occurrence in the metropolis. Other studies have also reported vegetation decline in Lagos (e.g., Abiodun et al. 2005; Babalola and Akinsanola 2016; Obiefuna et al. 2018). However, the small increase in the vegetation cover between 2013 and 2016 can be traced to grass and tree planting projects in the Lagos metropolis by the state government while the slight decrease in the water body area is as a result of the expansion of the residential area causing the inland water bodies to reduce in extent. Also, as earlier identified, another possible reason for decrease in water body could be the land reclamation projects within the study area.



**Table 10** Descriptive statistics of LST, NDVI and NDBI perland cover class

Year	Land cover class	*N	LST			NDVI			NDBI		
			Min	Max	Mean	Min	Max	Mean	Min	Max	Mean
2013	Bare land	12404	23.17	33.28	27.98	-0.03	0.8	0.45	-0.29	0.29	-0.05
	Built-up area	82466	23.03	33.93	28.8	-0.05	0.66	0.31	-0.28	0.25	-0.01
	Mixed vegetation	26300	23.09	30.78	25.45	0.06	0.82	0.62	-0.3	0.12	-0.15
	Wetland	45580	23.09	29.62	24.9	0.13	0.82	0.65	-0.32	0.03	-0.21
2016	Bare land	17784	21.67	31.64	25.89	0.05	0.66	0.41	-0.41	0.39	-0.09
	Built-up area	84271	22.52	31.66	27.45	0.06	0.55	0.26	-0.28	0.35	0.03
	Mixed vegetation	28519	21.39	29.71	23.63	0.11	0.67	0.53	-0.44	0.19	-0.21
	Wetland	36110	21.44	29.96	23.41	0.26	0.68	0.58	-0.45	0.03	-0.32
2019	Bare land	22100	21.93	33.17	26.32	0.04	0.72	0.44	-0.23	0.13	-0.08
	Built-up area	89862	20.12	33.15	28.08	0.05	0.61	0.27	-0.18	0.16	0.001
	Mixed vegetation	21007	19.64	29.14	24.77	0.06	0.73	0.53	-0.25	0.07	-0.14
	Wetland	33841	21.65	28.99	24.27	0.21	0.73	0.58	-0.26	0.00	-0.19

\*N – Number of sample points

The pattern of the land cover change was also examined through the transition matrices of the land cover types. The highest transitions noticed were the mixed vegetation to built-up area, and bare land to built-up area. The effect of these changes manifested in the distribution of LST, NDVI, and NDBI. The spatial pattern of the LST was similar to built-up areas. This validates the known premonitions that built-up areas are major contributors to increase in LST. This relationship has been corroborated by several authors

including Nse et al. (2020), Das and Angadi. (2020), Tepanosyan et al. (2020), Malik et al. (2019), Guha et al. (2018), and Obiefuna et al. (2021). According to Obiefuna et al. (2021), the main driver of land cover change is built-up area or urban development which had grown by over 770% since 1984 and as a result caused an increase in the mean LST over Lagos from 28.60 °C in 1984 to 30.76 °C in 2019. The low mean LST in the vegetated and wetland areas suggests relatively a higher rate of evapotranspiration and favoring

**Plate 2** A high-density urban area at Alakija roundabout along Lagos-Badagry expressway in Amuwo-Odofin ( source: Field survey, 2021)



**Plate 3** Some residential neighborhoods in Festac Town, Amuwo Odofin ( source: Alani et al. 2020)



of latent exchange between surface and atmosphere as compared with impervious surface like built-up and bare land areas (Alademomi et al. 2020). The NDBI results exhibited similar trend as LST and this is backed by the strong positive correlation between the indices for all the years: 2013 ( $r=0.84$ ), 2016 ( $r=0.87$ ), and 2019 ( $r=0.86$ ). The low NDVI observed over bare land and built-up area and high values seen over mixed vegetation and wetland is a common trend which has been reported by different NDVI-land cover studies (e.g., Han et al. 2019; Alademomi et al. 2020).

Generally, negative correlation coefficients are observed in the LST-NDVI and NDVI-NDBI relationship for all the years (Table 9). The similar behaviors exhibited in the relationship of LST and NDBI is expected because of the strong positive correlation between them. This agrees with Das et al. (2020) and Alexander (2020).

## Conclusion

The interrelationship between LST, NDVI, and NDBI within Amuwo Odofin LGA of Lagos state have been examined in this study in relation to the prominent land uses. The study observed that the pattern and values of the three parameters varied correspondingly in accordance to changes in land cover. The built-up area had the most significant change and as such, the LST increased considerably during the study period. Consequently, it can be concluded that increase in the built-up area is the major driver of LST, NDBI, and NDVI with an observed

relationship that NDBI and LST values increase with increase in built-up areas. Conversely, it was observed that there exists an inversely proportional relationship between NDVI and LST, and LST is directly proportional to NDBI

**Acknowledgements** The authors are grateful to the USGS for access to the Landsat imageries and the USGS EROS Centre for the Landsat spectral indices used in this research. Also, credits are due to the team that conducted the original research on the Landsat surface reflectance products (Masek et al., 2006; Vermote et al., 2016). The authors also thank the management of the Department of Surveying and Geoinformatics at the University of Lagos for providing a conducive research environment within which the study was conducted. Special thanks to Nkechi Onyiaqui and Julius Enakirerih for their help with acquiring field pictures.

## Declaration

**Conflict of interest** The authors declare no competing interests.

## References

- Abiodun OE, Olaleye JB, Dokai AN (2005) Land use change analyses in Lagos State from 1984 to 2005. *Spatial Information Processing II*, May 2011, 18–22
- Ajibola MO, Adewale BA, Ijase KC (2012) Effects of urbanisation on Lagos wetlands. *Int J Bus Soc Sci* 3(17):310–318
- Akinbobola A (2019) Simulating land cover changes and their impacts on land surface temperature in Onitsha, South East Nigeria. *Atmos Climate Sci* 09(02):243–263. <https://doi.org/10.4236/acs.2019.92017>

- Akinyemi FO, Ikanyeng M, Muro J (2019) Land cover change effects on land surface temperature trends in an African urbanizing dry-land region. *City Environ Interact* 4:100029. <https://doi.org/10.1016/j.cacint.2020.100029>
- Alademomi AS, Okolie CJ, Daramola OE, Agboola RO, Salami TJ (2020) Assessing the relationship of LST, NDVI and EVI with land cover changes in the Lagos Lagoon environment. *Quaestiones Geographicae* 39(3):87–109. <https://doi.org/10.2478/quageo-2020-0025>
- Alani RA, Ogunmoyela OM, Okolie CJ, Daramola OE (2020) Geospatial analysis of environmental noise levels in a residential area in Lagos. *Nigeria Noise Mapp* 2020(7):223–238. <https://doi.org/10.1515/noise-2020-0019>
- Alexander C (2020) Normalised difference spectral indices and urban land cover as indicators of land surface temperature (LST). *Int J Appl Earth Obs Geoinformation* 86(October 2019):102013
- Anderson JR (1971) Land use classification schemes used in selected recent geographic applications of remote sensing. *Photogramm Eng* 37(4):379–387
- Babalola OS, Akinsanola AA (2016) Change detection in land surface temperature and land use land cover over Lagos metropolis, Nigeria. *J Remote Sens GIS* 5(3). <https://doi.org/10.4172/2469-4134.1000171>
- Choudhury D, Das K, Das A (2019) Assessment of land use land cover changes and its impact on variations of land surface temperature in Asansol-Durgapur Development Region. *Egypt J Remote Sens Space Sci* 22(2):203–218. <https://doi.org/10.1016/j.ejrs.2018.05.004>
- Cummings S (2007) An analysis of surface temperature in San Antonio, Texas. Term Project. EES5053/ES4093: Remote Sensing, UTSA.
- Das S, Angadi DP (2020) Land use-land cover (LULC) transformation and its relation with land surface temperature changes: a case study of Barrackpore Subdivision, West Bengal, India. *Remote Sensing Applications: Society and Environment* 19(May):100322. <https://doi.org/10.1016/j.rsase.2020.100322>
- Das N, Mondal P, Sutradhar S, Ghosh R (2020) Assessment of variation of land use/land cover and its impact on land surface temperature of Asansol subdivision. *Egypt J Remote Sens Space Sci* S1110982320300272. <https://doi.org/10.1016/j.ejrs.2020.05.001>
- Deng Y, Wang S, Bai X et al (2018) Relationship among land surface temperature and LUCC, NDVI in typical karst area. *Sci Rep* 8:641. <https://doi.org/10.1038/s41598-017-19088-x>
- Fathizad H, Tazeh M, Kalantari S, Shojaei S (2017) The investigation of spatiotemporal variations of land surface temperature based on land use changes using NDVI in southwest of Iran. *J Afr Earth Sc* 134(2017):249–256. <https://doi.org/10.1016/j.jafrearsci.2017.06.007>
- Ferrelli F, Bustos M, Huamantincó-Cisneros M, Piccolo M (2015) Utilization of satellite images to study the thermal distribution in different soil covers in Bahía Blanca city (Argentina). *Revista De Teledetección* 44:31–42
- Grigoras G, Uritescu B (2019) Land use/land cover changes dynamics and their effects on surface urban heat island in Bucharest, Romania. *Int J Appl Earth Obs Geoinf* 80(February):115–126. <https://doi.org/10.1016/j.jag.2019.03.009>
- Guha S et al (2018) Analytical study of land surface temperature with NDVI and NDBI using Landsat 8 OLI and TIRS data in Florence and Naples city, Italy." *Eur J Remote Sens* 51(1):667–678
- Guha S, Govil H, Gill N, Dey A (2020) Analytical study on the relationship between land surface temperature and land use/land cover indices. *Ann GIS* 26(2):201–216. <https://doi.org/10.1080/19475683.2020.1754291>
- Han JC, Huang Y, Zhang H, Wu X (2019) Characterization of elevation and land cover dependent trends of NDVI variations in the Hexi region, northwest China. *J Environ Manag* 232(November 2018):1037–1048. <https://doi.org/10.1016/j.jenvman.2018.11.069>
- Hua AK, Ping OW (2018) The influence of land-use/land-cover changes on land surface temperature: a case study of Kuala Lumpur metropolitan city. *Eur J Remote Sens* 51(1):1049–1069. <https://doi.org/10.1080/22797254.2018.1542976>
- Jaber SM (2019) On the relationship between normalized difference vegetation index and land surface temperature: MODIS-based analysis in a semi-arid to arid environment. *Geocarto Int* 0(1010–6049):1–19. <https://doi.org/10.1080/10106049.2019.1633421>
- Kabano P, Lindley S, Harris A (2021) Evidence of urban heat island impacts on the vegetation growing season length in a tropical city. *Land scape and Urban Plan* 206:103989
- L3Harris Geospatial (2020). Gram-Schmidt pan sharpening. <https://www.l3harrisgeospatial.com/docs/gramschmidtspectralsharpening.html#:~:text=ENVI%20performs%20Gram%2DSchmidt%20spectral,lower%20spatial%20resolution%20spectral%20bands.&text=Swapping%20the%20high%20spatial%20resolution, the%20pan%2Dsharpened%20spectral%20bands>. Accessed 4 Aug 2021
- Lagos Bureau of Statistics (2019) Abstract of local government statistics. <https://mepb.lagosstate.gov.ng/wp-content/uploads/sites/29/2020/08/Abstract-of-Local-Government-Statistics-Y2019.pdf>. Accessed 30 Sept 2020
- Malik MS, Shukla JP, Mishra S (2019) Relationship of LST, NDBI and NDVI using landsat-8 data in Kandaihimmat watershed, Hoshangabad. *India Indian J Geo-Marine Sci* 48(1):25–31
- Marzban F, Sodoudi S, Preusker R (2018) The influence of land-cover type on the relationship between NDVI–LST and LST–Tair. *Int J Remote Sens* 39(5):1377–1398. <https://doi.org/10.1080/01431161.2017.1402386>
- Masek JG, Vermote EF, Saleous NE, Wolfe R, Hall FG, Huemmrich KF, Gao F, Kutler J, Lim T-K (2006) A Landsat surface reflectance data set for North America, 1990–100. *IEEE Geosci Remote Sens Lett* 3:68–72
- Nse OU, Okolie CJ, Nse VO (2020) Dynamics of land cover, land surface temperature and NDVI in Uyo Capital City. *Nigeria Sci Afr* 10(2020):00599. <https://doi.org/10.1016/j.sciaf.2020.e00599>
- Nwilo PC, Olayinka DN, Okolie CJ, Emmanuel EI, Orji MJ, Daramola OE (2020) Impacts of land cover changes on desertification in northern Nigeria and implications on the Lake Chad Basin. *J Arid Environ* 181(April):104190. <https://doi.org/10.1016/j.jaridenv.2020.104190>
- Obiefuna JN, Nwilo PC, Atagbaza AO, Okolie CJ (2013) Spatial changes in the wetlands of Lagos/Lekki Lagoons of Lagos. *Niger J Sustain Dev* 6(7):123–133. <https://doi.org/10.5539/jsd.v6n7p123>
- Obiefuna JN, Nwilo PC, Atagbaza AO, Okolie CJ (2013) Land cover dynamics associated with the spatial changes in the Wetlands of Lagos/Lekki Lagoon system of Lagos. *Niger J Coast Res* 29(3):671–679. <https://doi.org/10.2112/JCOAS-TRES-D-12-00038.1>
- Obiefuna JN, Nwilo PC, Okolie CJ, Emmanuel EI, Daramola O (2018) Dynamics of land surface temperature in response to land cover changes in Lagos metropolis. *Niger J Environ Sci Technol* 2(2):148–159. <https://doi.org/10.36263/nijest.2018.02.0074>
- Obiefuna JN, Okolie CJ, Nwilo PC, Daramola OE, Isiofia LC (2021) Potential influence of urban sprawl and changing land surface temperature on outdoor thermal comfort in Lagos State. *Nigeria Quaestiones Geographicae* 40(1):5–23. <https://doi.org/10.2478/quageo-2021-0001>
- Oguz H (2013) LST calculator: A program for retrieving land surface temperature from Landsat TM/ETM+ imagery. *Environ Eng Manag J* 12(3):549–555
- Qin Z, Karnieli A, Berlinier P (2001) A mono-window algorithm for retrieving land surface temperature from Landsat TM data and its



- application to the Israel-Egypt border region. *Int J Remote Sens* 22(18):3719–3746
- Schott JR, Volchok WJ (1985) Thematic mapper thermal infrared calibration. *Photogramm Eng Remote Sens* 51:1351–1357
- Siqi J, Yuhong W (2020) Effects of land use and land cover pattern on urban temperature variations: a case study in Hong Kong. *Urban Climate* 34(August):100693. <https://doi.org/10.1016/j.uclim.2020.100693>
- Tepanosyan G, Muradyan V, Hovsepyan A, Pinigin G, Medvedev A, Asmaryan S (2020) Studying spatial-temporal changes and relationship of land cover and surface urban heat island derived through remote sensing in Yerevan, Armenia, building and environment (2020) <https://doi.org/10.1016/j.builde.2020.107390>.
- UNFPA (2020) Delivering in a pandemic annual report 2020
- USGS (2015) Landsat 8 (L8) Data users handbook, version 1.0. L8SDS-1574. Department of the Interior, U.S. Geological Survey
- Vermote E, Justice C, Claverie M, Franch B (2016) Preliminary analysis of the performance of the Landsat 8/OLI land surface reflectance product. *Remote Sens Environ* 185:46–56
- Weng Q, Lu D, Schubring J (2004) Estimation of land surface temperature – vegetation abundance relationship for urban heat island studies. *Remote Sens Environ* 89(4):467–483
- Wukelic GE, Gibbons DE, Martucci LM, Foote HP (1989) Radiometric calibration of Landsat thematic mapper thermal band. *Remote Sens Environ* 28:339–347
- Yusuf KA, Oluwole S, Abdusalam IO, Adewusi GR (2013) Spatial patterns of urban air pollution in an industrial estate, Lagos, Nigeria spatial patterns of urban air pollution in an industrial estate, Lagos. *Niger Int J Eng Inventions* 2(4):1–9
- Zareie S, Khosravi H, Nasiri A (2016) Derivation of land surface temperature from Landsat thematic mapper (TM) sensor data and analyzing relation between land use changes and Surface Temperature. *Solid Earth Discuss.* 10.5194/se-2016-22,201
- Zha Y, Gao J, Ni S (2003) Use of normalized difference built-up index in automatically mapping urban areas from TM imagery. *Int J Remote Sens* 24(3):583–594. <https://doi.org/10.1080/01431160304987>